International Journal of Naval Architecture and Ocean Engineering 12 (2020) 943–956

Contents lists available at ScienceDirect

International Journal of Naval Architecture and Ocean Engineering

journal homepage: http://www.journals.elsevier.com/international-journal-of-naval-architecture-and-ocean-engineering/

Control system design for vessel towing system by activating rudders of the towed vessel

Dong-Hun Lee, Soumayya Chakir, Young-Bok Kim*, Duc-Quan Tran**

Department of Mechanical System Engineering, The Graduate School, Pukyong National University, Nam-gu, Busan, South Korea

ARTICLE INFO

Article history:
Received 4 July 2020
Received in revised form
26 November 2020
Accepted 30 November 2020
Available online 14 December 2020

Keywords:
Towed vessel
Towing ship
Course stability
Rudder
Maneuverability
Leader-follower
Nonlinear model
Back-stepping control

ABSTRACT

In this study, the motion control problem of the vessel towed by a towing ship (tugboat) is considered. The non-powered towed ship is dragged by the towing ship. Even though the towed ship is equipped with propulsion systems, they cannot be used at low or constant speeds due to safety issues. In narrow canals, rivers, and busy harbor areas especially, where extreme tension is required during towing operation, the course stability of the towed vessel depends on the towing ship. Therefore, the authors propose a new control strategy in which the rudder system of the towed vessel is activated to provide its maneuverability. Based on the leader-follower system configuration, a nonlinear mathematical model is derived and a back-stepping control is designed. By simulation and experiment results with a comparison study, the usefulness and effectiveness of the proposed strategy are validated.

© 2020 Society of Naval Architects of Korea. Production and hosting by Elsevier B.V. This is an open access article under the CC BY-NC-ND license (http://creativecommons.org/licenses/by-nc-nd/4.0/).

1. Introduction

The development of control and measurement technology has made remarkable results regardless of its application areas and subjects. Especially, applications to the marine field are increasing and more recently extending to the area where autonomous navigation is possible. Recently, many control technologies had begun to be applied in ship motion control problems. The main issue was the problem of path control at a low or constant speed. Therefore, complex and intricate research studies have been carried out.

- Background:

In the previous research studies, a given goal was to maintain the right path in the wide ocean (Dong et al., 2015; Fossen, 2002; Lopez and Rubio, 1992; Machiel et al., 2011; Fang M.C., Lee Z.Y., 2016; Wang et al., 2020; Yamato et al., 1990; Zhang et al., 1999; Zwierzewicz, 1999). Also, Wang et al. (2019) investigated the path following a problem of a surface vessel sailing in the restricted water. In other words, using the main propulsion device and the rudders, the sailing technologies have been developed.

Also, more sophisticated ship motion control strategies are necessary when the ship starts approaching the harbor. To partially overcome the stability problem of the berthing process, several solutions were proposed. In these studies, the ship is moved in parallel to the seawall with only the side thrusters (Bui et al., 2010, 2011; Bui and Kim, 2011; Tran et al., 2014, 2018; Lee et al., 2000). The objective of these studies is to improve the stability of the docking operation at the final stage or restricted maneuvering environment. The various ship motion control methods and techniques described above are implemented by installing the active control devices on the controlled vessel. In other words, it is natural that the motion control system is installed on the controlled vessel itself.

- Problem formulation:

On the sea, non-powered ships (such as barges) are frequently used for transporting cargos and moving large structures from the

* Corresponding author.
** Corresponding author.
E-mail addresses: iottoi@pukyong.ac.kr (D.-H. Lee), soumayya.chakir@gmail.com (S. Chakir), kpjiwoo@pknu.ac.kr (Y.-B. Kim), tranducquan@tnut.edu.vn (D.-Q. Tran).

Peer review under responsibility of Society of Naval Architects of Korea.

https://doi.org/10.1016/j.ijnaoe.2020.11.008

2092-6782/© 2020 Society of Naval Architects of Korea. Production and hosting by Elsevier B.V. This is an open access article under the CC BY-NC-ND license (http://creativecommons.org/licenses/by-nc-nd/4.0/).

shipyard to other places; these barge-type vessels are dragged by tugboats. In some cases, such as going through canals, narrow rivers, or working on the busy harbor area, the ships with propulsion systems are towed by tugboats under a non-powered state as shown in Fig. 1.

In the cases abovementioned, the tugboat leads and controls the towed vessel. However, it is difficult to make the towed vessels follow the tugboat's moving route due to the loss of maneuverability. Moreover, safe maneuvering may be impossible in harsh sea conditions.

About this issue, Fitriadhy et al. (2013) gave an interesting proposal with a mathematical model and course stability analysis. The obtained model presents the dynamics of the tugboat and the non-powered barge subjected to wind attacks. The result shows that the stability of the towing system strongly depends on the wind attack angle and the towing rope length. Additionally, Tran et al. (2019) presented the simulation results based on the simplified linear model of the towed vessel. However, system stability and dynamic analysis were obtained using the linearized model.

Using active strategies is proven to be necessary to guarantee system stability and maneuverability. If we insist on using conventional and inactive methods, stable and good sailing performances could not be preserved. Severe accidents may eventually occur due to wave disturbances and complicated maneuvering conditions caused by other vessels passing by. Needless to mention, if the towed vessel deviates from the path of the tugboat, collision possibility with other ships may increase.

- Contributions:

In this study, a new method to solve the abovementioned problem is discussed. To facilitate the maneuverability of non-powered vessels, the authors introduce a novel strategy based on the leader-follower concept. It is a control system method for the towed and towing vessel system shown in Fig. 2. Therefore, giving minimal function to the powerless towed vessel provides it with a controllable rudder.

Practically, the rudder or portable propulsion system can be additionally provided for the non-powered vessels (such as barge ships) and controlled. Furthermore, the ships sailing in narrow and restricted waters can be controlled by a remote control system. Therefore, by installing rudders at the rear side of the towed vessel, the restoring moments increase due to the lateral hydrodynamic force when the drift angle occurs. Without a doubt and based on the precedent analysis, active rudders are necessary to provide system stability and maneuverability.



Fig. 1. Photo of non-powered ship docking operation with the assistance of tugboats.

In this study, the nonlinear dynamic response of a vessel towing system is investigated. The motion of the towing tugboat is described by a dynamic model. The motion of the towed vessel is described by a nonlinear model derived from the relationship between the towing tugboat and the towed vessel. Nonlinear controllers for the tugboat and the towed vessel are designed independently without linearization. A comparison study is conducted through simulation and experiment using the pilot model ship, and the results are given to evaluate the control performance.

Thus, the contributions of this paper are listed as follows:

Modeling of the vessel towing system;
Design of a nonlinear PID controller for the towing tugboat;
Design of a nonlinear back-stepping control scheme for the towed vessel;
Stability analysis;
Verification of study results by simulation and experiment.

Finally, the remainder of this article is organized as follows. Section 2 discusses the modeling of the vessel towing system while rudders of the towed vessel are active. Section 3 presents the analytical design of motion control of the vessel towing system. Setting a pilot model, identification of parameters, and simulation results are discussed in section 4. Experiment results are discussed in section 5. Conclusions will be drawn in section 6.

2. System modeling

To design the control system, having a mathematical model that describes the dynamics of the system is compulsory. As shown in Fig. 3, the towed vessel does not have any self-thrust force based on the assumption given before. Moreover, it is assumed that two rudders are adequately installed at arbitrary positions. For maneuverability and compatibility reasons the number of rudders in this study was limited to two rudders to keep the robust stability of the towed vessel. However, there is no constraint on the number of rudders, and it is possible to activate and use them to improve sailing stability in the real towing operation.

The parameters illustrated in Fig. 3 are denoted as follows:

(x_0, y_0): coordinates of the connecting point at the towing vessel;

(x_1, y_1): gravity center of the towing vessel;

(x_2, y_2): gravity center of the towed vessel;

ψ_2: heading angle of the towed vessel;

γ: relative angle made by the target position and the control position;

$\delta_i (i = 1, 2)$: rudder rotation angle;

l_r: rope length for connecting the towing tugboat and towed vessel. It is assumed that the length

change of l_r is sufficiently small and the mass of the rope is relatively small;

l_T: distance from the gravity center to the rope connecting point of the towed vessel;

l_s: distance from the center of rudder #1, #2 to the gravity center of the towed vessel;

l_{ss}: distance from the center of rudder #1, #2 to the gravity center of the towed vessel in the surge direction.

2.1. Towing tugboat dynamics

In this study, surge, sway, and yaw motions of towing tugboat in the horizontal plane are taken into consideration. Then the 3-DOF equation of motions is derived adequately as follows (Fossen, 2002):

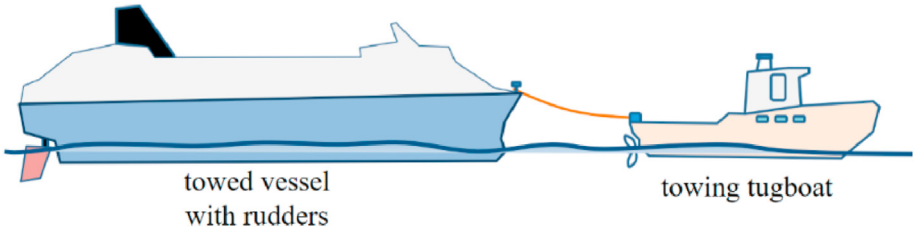


Fig. 2. Schematics of the controlled system with active rudders.

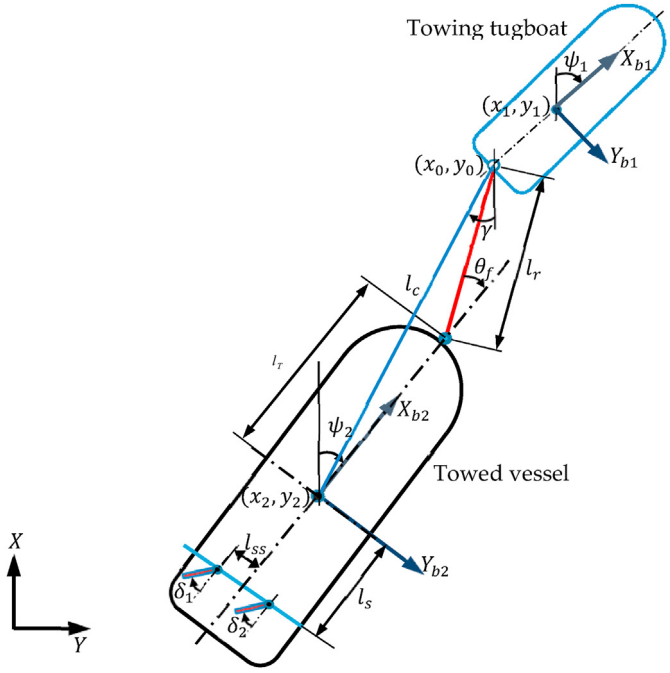


Fig. 3. Configuration of the vessel towing system.

$$\dot{\eta}_1 = R(\psi_1)\nu_1 \tag{1}$$

$$M_1\dot{\nu}_1 + D_1\nu_1 = \tau_1 - \tau_{rope} \tag{2}$$

where $\eta_1 = [x_1, y_1, \psi_1]^T \in R^3$ represents the position (x_1, y_1) and the heading angle ψ_1 in the earth-fixed frame. $\nu_1 = [u_1, v_1, r_1]^T \in R^3$ describes the surge, sway, and yaw rate of ship motion in the body-fixed frame. $\tau_1 = [\tau_{x1} \quad \tau_{y1} \quad \tau_{\psi 1}]^T$ is thrust vector and denotes surge force, sway force, and yaw moment around the center of gravity of the towing tugboat. the vector $\tau_1 = [\tau_{x1} \quad \tau_{y1} \quad \tau_{\psi 1}]^T$ denotes surge force, sway force, and yaw moment made by the towing tugboat. The rotation matrix, Eq. (3), in the heading direction $R(\psi_1)$ describes the kinematic equation of motion.

$$R(\psi_1) = \begin{bmatrix} \cos\psi_1 & -sin\psi_1 & 0 \\ sin\psi_1 & \cos\psi_1 & 0 \\ 0 & 0 & 1 \end{bmatrix} \tag{3}$$

Moreover, $M_1 \in R^{3\times3}$ is the inertia matrix including the added mass as described as Eq. (4). For control application purposes, the vessel's motion is restricted to low frequency. The wave frequency is assumed to be independent of added inertia which implies $\dot{M}_1 = 0$.[3]

$$M_1 = \begin{bmatrix} m_1 - X_{\dot{u}1} & 0 & 0 \\ 0 & m_1 - Y_{\dot{v}1} & -Y_{\dot{r}1} \\ 0 & -N_{\dot{v}1} & I_{z1} - N_{\dot{r}1} \end{bmatrix} \tag{4}$$

Finally, $D_1(\nu_1) \in R^{3\times3}$ is the damping matrix and it is a function of the relative velocity between the vessel and the current. In low-speed applications, the damping matrix is assumed to be constant (Fossen, 2002), and defined as follows

$$D_1 = \begin{bmatrix} -X_{u1} & 0 & 0 \\ 0 & -Y_{v1} & -Y_{r1} \\ 0 & -N_{v1} & -N_{r1} \end{bmatrix} \tag{5}$$

The parameters presented in Eqs. (4) and (5) are summarized as follows:

m_1: body mass of towing tugboat.
I_{z1}: the moment of inertia about z axes.
$X_{\dot{u}_1}, Y_{\dot{v}_1}, Y_{\dot{r}_1}$: additional mass.
$N_{\dot{v}1}, N_{\dot{r}1}$: the additional moment of inertia.
u_1, v_1: x_1, y_1 direction velocity component.

2.2. Towed vessel dynamics

Same as the description of the towing tugboat, the 3-DOF equation of the towed vessel dynamics are derived as follows:

$$\dot{\eta}_2 = R(\psi_2)\nu_2 \tag{6}$$

$$M_2\dot{\nu}_2 + D_2\nu_2 = \tau_2 \tag{7}$$

where $\tau_2 = [\tau_{x2} \quad \tau_{y2} \quad \tau_{\psi 2}]^T$ denotes surge force, sway force, and yaw moment. The actual actuation τ_2 of the towed vessel is generated by the traction force of the rope and the rudders. And $R(\psi_2), M_2, D_2$ are defined, respectively, in the same manner as $R(\psi_1)$, M_1, D_1.

As shown in Fig. 3, we consider that the connecting point (x_0, y_0) on the tugboat is the tracking target of the towed vessel, since the leading tugboat tows the controlled vessel with a rope. It means that the tracking route is generated automatically by the connecting point of the rope of the towing vessel. Then, the towed vessel motion can be solved by using the weather optimal positioning control (WOPC) method (Fossen, 2002; Fitriadhy et al., 2013) which is a useful method for deriving a solution of this issue.

The cartesian coordinates (x_2, y_2) can be represented using the polar coordinates, and are given as follows:

$$x_2 = x_0 + l_c\cos\gamma \tag{8}$$

$$y_2 = y_0 + l_c\sin\gamma \tag{9}$$

where,

$$l_c = \sqrt{(x_2 - x_0)^2 + (y_2 - y_0)^2} \tag{10}$$

$$\gamma = atan2(y_2 - y_0, x_2 - x_0) \tag{11}$$

The derivatives of Eqs. (8) and (9) are as follows:

$$\dot{x}_2 = \dot{x}_0 + \dot{l}_c \cos\gamma - l_c \sin\gamma\dot{\gamma} \tag{12}$$

$$\dot{y}_2 = \dot{y}_0 + \dot{l}_c \sin\gamma + l_c \cos\gamma\dot{\gamma} \tag{13}$$

From Eq. (12) and Eq. (13), $\eta_2 = [x_2, y_2, \psi_2]^T \in R^3$ can be expressed as

$$\dot{\eta}_2 = \begin{bmatrix} \cos\gamma & -sin\gamma & 0 \\ sin\gamma & \cos\gamma & 0 \\ 0 & 0 & 1 \end{bmatrix} \begin{bmatrix} 1 & 0 & 0 \\ 0 & l_c & 0 \\ 0 & 0 & 1 \end{bmatrix} \begin{bmatrix} \dot{l}_c \\ \dot{\gamma} \\ \dot{\psi}_2 \end{bmatrix} + \begin{bmatrix} 1 & 0 \\ 0 & 1 \\ 0 & 0 \end{bmatrix} \begin{bmatrix} \dot{x}_0 \\ \dot{y}_0 \end{bmatrix} \tag{14}$$

We define the state vectors as:

$$p_0 = \begin{bmatrix} x_0 \\ y_0 \end{bmatrix}, \; x = \begin{bmatrix} l_c \\ \gamma \\ \psi_2 \end{bmatrix} \tag{15}$$

Then the new kinematic relationship can be written in terms of the vectors p_0 and x:

$$\dot{\eta}_2 = R(\gamma)H(l_c)\dot{x} + L\dot{p}_0 \tag{16}$$

where,

$$R(\gamma) = \begin{bmatrix} \cos\gamma & -sin\gamma & 0 \\ sin\gamma & \cos\gamma & 0 \\ 0 & 0 & 1 \end{bmatrix} H(l_c) = \begin{bmatrix} 1 & 0 & 0 \\ 0 & l_c & 0 \\ 0 & 0 & 1 \end{bmatrix} L = \begin{bmatrix} 1 & 0 \\ 0 & 1 \\ 0 & 0 \end{bmatrix} \tag{17}$$

Using Eq. (16), Eq. (6) can be written as the following differential equation

$$\dot{x} = T(x)\nu_2 - T(x)R^T(\psi_2)L\dot{p}_0 \tag{18}$$

where $T(x)$ is

$$T(x) = H^{-1}(l_c)R^T(\gamma)R(\psi_2) \tag{19}$$

For the convenience of expression, we define $T(x) = T, H(l_c) = H, M_2(\nu) = M_2, D_2(\nu) = D_2$. Therefore, Eq. (18) can be represented as follows:

$$\nu_2 = T^{-1}\dot{x} + R^T(\psi_2)L\dot{p}_0 \tag{20}$$

And, the time differentiation of Eq. (20) is

$$\dot{\nu}_2 = T^{-1}\ddot{x} + \dot{T}^{-1}\dot{x} + R^T(\psi_2)L\ddot{p}_0 + \dot{R}^T(\psi_2)L\dot{p}_0. \tag{21}$$

The resulting expressions from Eq. (18), Eq. (20), and Eq. (21), the towed vessel model Eq. (7) becomes

$$M_x\ddot{x} + D_x\dot{x} = T^{-T}\left[q\left(\nu, x, \dot{p}_0, \ddot{p}_0\right) + \tau_2\right], \tag{22}$$

where

$$q\left(\nu_2, x, \dot{p}_0, \ddot{p}_0\right) = -M_2R^T(\psi_2)L\ddot{p}_0 - M_2\dot{R}^T(\psi_2)L\dot{p}_0 - D_2R^T(\psi_2)L\dot{p}_0, \tag{23}$$

$$M_x = T^{-T}M_2T^{-1}, \; D_x = T^{-T}D_2T^{-1} + T^{-T}M_2\dot{T}^{-1}. \tag{24}$$

3. Control system design

The goal of the control system design is to achieve the desirable tracking performance of the towed vessel with course stability. The positions and heading angles of both towing and towed vessels should follow the desired trajectory. Naturally, the towing tugboat is controlled such that the desired trajectory of the towed vessel is made. Furthermore, the towed vessel should be controlled to track accurately the trajectory generated by the towing tugboat regardless of its direction. Based on these objectives, the authors designed two different control systems.

3.1. Control system design of the towing tugboat

The control structure of the towing tugboat is shown in Fig. 4. The nonlinear PID controller is derived as

$$\tau_{PID} = K_{P1}(\eta_1 - \eta_{d1}) + K_{D1}\left(\dot{\eta}_1 - \dot{\eta}_{d1}\right) + K_{I1}\int_0^t (\eta_1 - \eta_{d1})dt \tag{25}$$

where η_1 is the actual motion vector, and η_{d1} is the desired motion vector of the surge and the sway position, as well as the yaw angle.

3.2. Control system design for the towed vessel

The main objective of the control design for the towing system is controlling the towed vessel to go after the towing tugboat. To achieve this objective, we consider three requirements.

The first requirement is keeping the distance between the two vessels to be constant. And, the second is controlling the relative angle made between the target position and the control position to be $\gamma_d = \psi_1 + \pi$. Finally, the last requirement is controlling the heading angle of the towed vessel to be $\psi_{2d} = \psi_1$.

Based on the aforementioned, the authors design a nonlinear control law based on the back-stepping technique. Then, we need to design the control law τ_2 such that the system in Eq. (26) is stable.

$$M_x\ddot{x} + D_x\dot{x} = T^{-T}\tau_2 + T^{-T}q \tag{26}$$

If we define the reference trajectory vector as $x_{\boldsymbol{d}} = [l_{cd} \;\; \gamma_d \;\; \psi_{2d}]^T \in R^3$, the control design process based on the nonlinear control framework is summarized as follows.

Step 1: Definition of the error variables

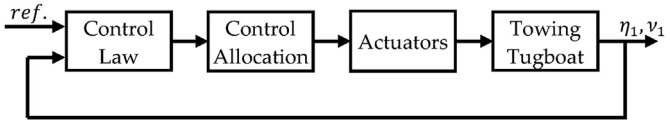


Fig. 4. General control configuration of the towing tugboat.

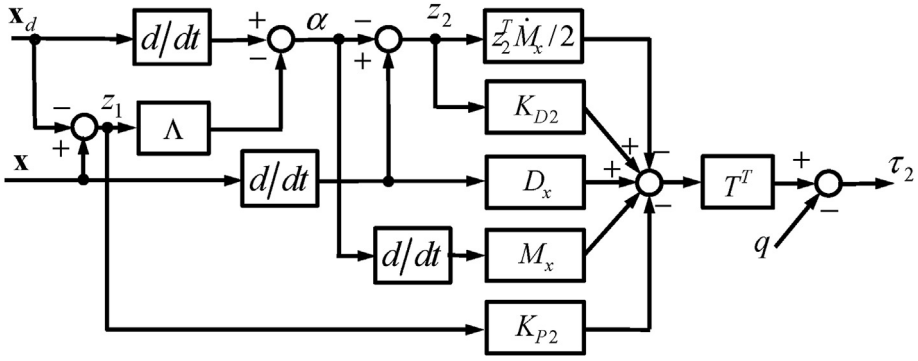
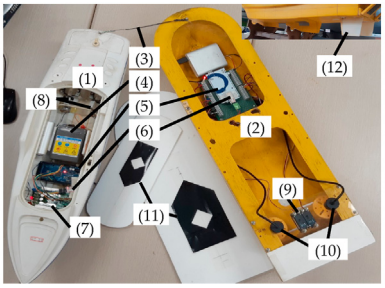
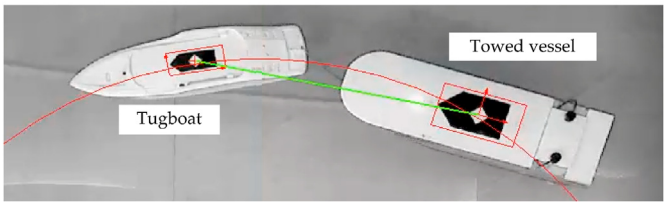


Fig. 5. Configuration of the designed back-stepping controller for the towed vessel.



(a) towing vessel system experimental apparatus



(b) towing vessel system in the basin

Fig. 6. The leader-follower experiment apparatus.

Table 1
Experimental apparatus installed on two vessels.

No.	Apparatus name	No.	Apparatus name
1	Tugboat (towing vessel)	7	DC motor controller H-bridge drive
2	Towed vessel	8	DC motor propeller
3	Rope	9	Rudder controller by servo motor
4	Battery power	10	Encoder
5	Arduino Mega 2560	11	Template image
6	RF module HC-06	12	Rudder (76mmx61mm)

$$z_1 = x - x_d \tag{27}$$

$$z_2 = \dot{x} - \alpha \tag{28}$$

where z_1 is the tracking error dynamics and α is the stabilizing vector:

$$\alpha = \dot{x}_d - \Lambda z_1 \tag{29}$$

and $\Lambda(>0)$ is a positive definite diagonal matrix.

From Eq. (28) and Eq. (29), the time derivative of z_1 is represented as follows:

$$\dot{z}_1 = \dot{x} - \dot{x}_d = z_2 - \Lambda z_1 \tag{30}$$

We define a Lyapunov function candidate and its time derivative respectively as in Eq. (31) and Eq. (32).

$$V_1 = \frac{1}{2} z_1^T K_{P2} z_1 \tag{31}$$

$$\dot{V}_1 = z_1^T K_{P2} \dot{z}_1 = -z_1^T K_{P2} \Lambda z_1 + z_1^T K_{P2} z_2 \tag{32}$$

where $K_{P2}(>0)$ is a diagonal matrix.

Step 2: From Eq. (28), the following expressions are obtained.

$$\dot{x} = z_2 + \alpha \tag{33}$$

$$\ddot{x} = \dot{z}_2 + \dot{\alpha} \tag{34}$$

This implies that the towed vessel motion, described in Eq. (26), can be expressed in terms of z_2 and α from Eq. (33) and Eq. (34). The resulting expression is given as follows

$$M_x \dot{z}_2 + D_x z_2 = T^{-T}\tau_2 + T^{-T} q - M_x \dot{\alpha} - D_x \alpha \tag{35}$$

We define an additional Lyapunov function candidate

$$V_2 = V_1 + \frac{1}{2} z_2^T M_x z_2 \tag{36}$$

And its time derivative yields

$$\dot{V}_2 = \dot{V}_1 + z_2^T M_x \dot{z}_2 + \frac{1}{2} z_2^T \dot{M}_x z_2 \tag{37}$$

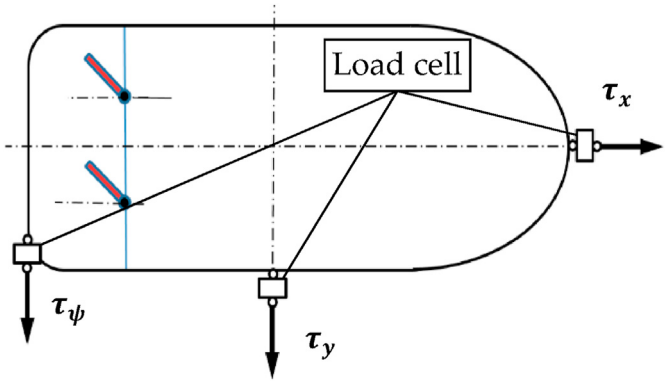


Fig. 7. Placement of load cells used for parameter identification.

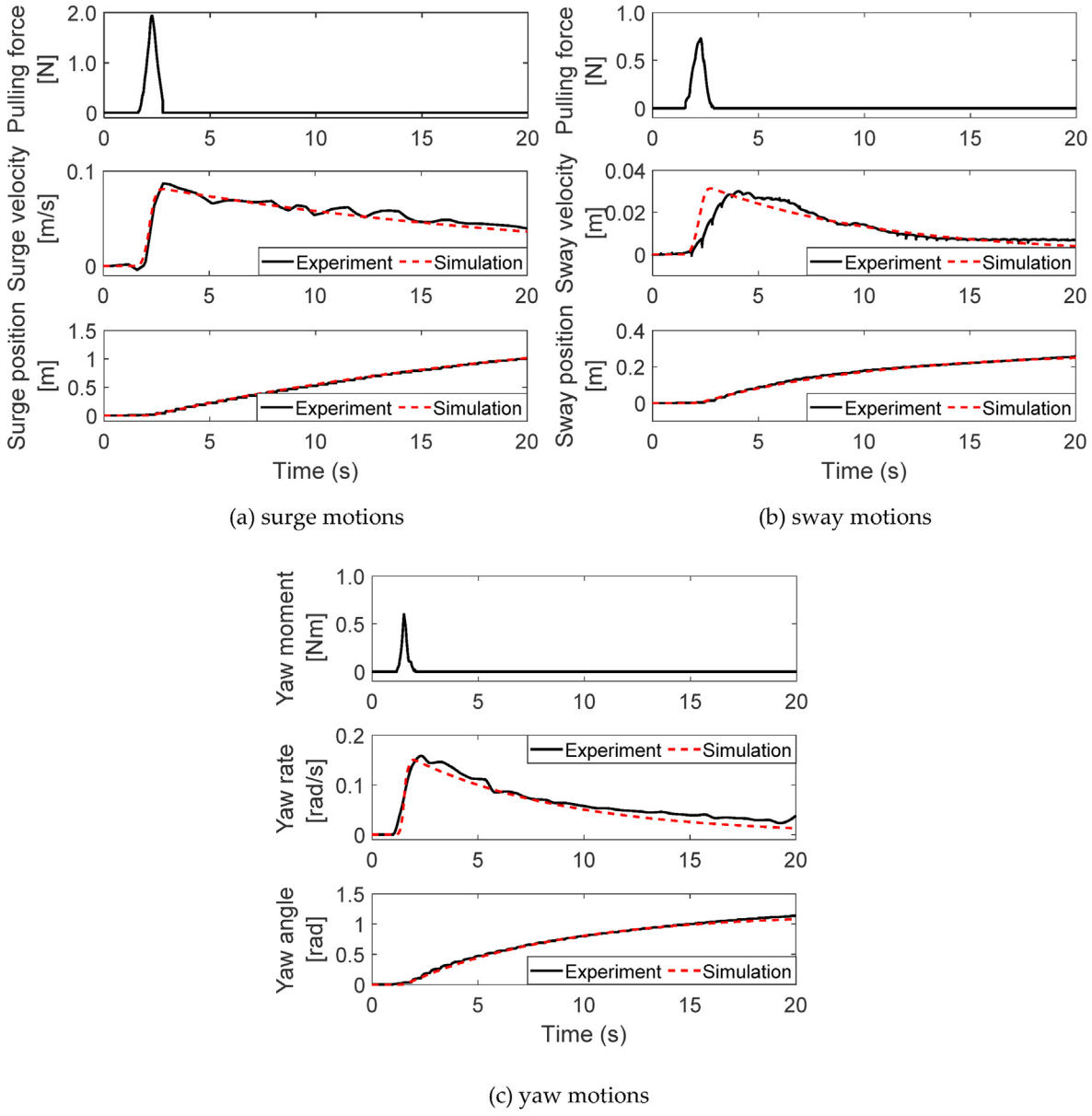


Fig. 8. The pulling force and towed vessel motions resulting from pulling the towed vessel.

Moreover, inserting Eq. (32) and Eq. (35) in Eq. (37) results in a new expression of the time derivative of V_2 given as follows

$$\dot{V}_2 = -z_1^T K_{P2} \Lambda z_1 + z_1^T K_{P2} z_2 + z_2^T \left[T^{-T}\tau_2 + T^{-T} q - M_x \dot{\alpha} - D_x \alpha - D_x z_2 \right] + \frac{1}{2} z_2^T \dot{M}_x z_2 \tag{38}$$

To satisfy the condition $\dot{V}_2 < 0$, the control law should be chosen as

$$T^{-T}\tau_2 = -T^{-T} q + M_x \dot{\alpha} + D_x \dot{x} - K_{P2} z_1 - K_{D2} z_2 - \frac{1}{2} z_2^T \dot{M}_x z_2 \tag{39}$$

where $K_{D2}(>0)$ is a diagonal matrix. Then, Eq. (38) can be expressed using Eq. (39) as follows

$$\dot{V}_2 = -z_1^T K_{P2} \Lambda z_1 - z_2^T K_{D2} z_2 < 0 \tag{40}$$

Then, Eq. (40) implies that z_1 and z_2 are bounded. Also, the uniformly continuous property of $\dot{V}_2$ can be shown easily by deriving time derivatives of $\dot{V}_2$. Therefore, according to Barbalat's lemma, it can be obtained that $\dot{V}_2 \to 0$ as $t \to \infty$. Then, it is clear that the system Eq. (35) is globally asymptotically stable with the control law of Eq. (39). Therefore, the tracking error and its derivative converge to zero. Finally, the designed control vector is obtained as

$$\tau_2 = -q + T^T \left[M_x \dot{\alpha} + D_x \dot{x} - K_{P2} z_1 - K_{D2} z_2 - \frac{1}{2} z_2^T \dot{M}_x z_2 \right] \tag{41}$$

Additionally, the configuration of the proposed back-stepping control system for the towed vessel can be illustrated as Fig. 5.

4. Simulation

In the following sections, setting up the experimental apparatus, parameter identification of the pilot model of the towing system is represented. The performance and effectiveness of the proposed strategy are validated through simulation and experiment results.

4.1. Hydrodynamic coefficients estimation

The experiments were carried out in the Marine Cybernetics Laboratory located at the Department of Mechanical System Engineering, Pukyong National University using a pilot model. The towing tugboat has a mass of 1.977 [kg], length of 0.73 [m] and breadth of 0.195 [m]. The towed vessel has a mass of 3.456[kg], length of 0.79 [m] and breadth of 0.235 [m]. They are shown in Fig. 6. Two main propellers are installed in the towing tugboat, and they are controlled by DC motors. While two rudders are installed in the towed vessel, their angles are controlled by servo motors. There is not any actuator on the towed vessel. The towed vessel is pulled by the tugboat using a rope connecting the two vessels. The rope has a length of 0.21 [m], and the distance between the tugboat and the towed vessel is as 0.95 [m]. If connection points are collinear the rope is stretched. The rudder has a length of 0.076 [m], breadth of 0.061 [m], and thickness of 0.005 [m]. The rudder positions are measured as $l_r = 0.6[m]\ l_T = 0.3[m]\ l_s = 0.27[m], l_{ss} = 0.1[m]$. And, the basin has a length of 5.6 [m], breadth of 3.0 [m], and a water depth of 0.6 [m].

Table 1 introduces some equipment used in setting up the experimental apparatus. The control system is executed on a host onshore computer.

Besides, a USB camera is attached to the ceiling to capture the vessel motions. The image data (vessel motions) taken by the camera is transferred to the host onshore computer. Using the pattern-matching machine vision technique, vessel motions (surge, sway motions, and yaw angle) are calculated in real-time (Kehtarnavaz and Kim, 2005; Kawai et al., 2009, 2012; Yoon et al., 2010; Kunimitsu et al., 2004).

Then the calculated positions and yaw angles are sent to the control system. The transferring mean between the computer and two vessels is via RF (radio frequency technique).

For simplicity, it is assumed that the vessel has homogeneous mass distribution, xz and yz are plan symmetry, as well as the center of gravity coinciding with the center of geometry. This allows for the following nominal inertia and damping matrices:

$$M_i = \begin{bmatrix} m_i - X_{\dot{u}i} & 0 & 0 \\ 0 & m_i - Y_{\dot{v}i} & 0 \\ 0 & 0 & I_{zi} - N_{\dot{r}i} \end{bmatrix} \tag{42}$$

$$D_i = \begin{bmatrix} -X_{ui} & 0 & 0 \\ 0 & -Y_{vi} & 0 \\ 0 & 0 & -N_{ri} \end{bmatrix},\ i = 1, 2. \tag{43}$$

The dynamics of the tugboat and towed vessel in the surge, sway, and yaw direction are decoupled based on this assumption. Substituting (42) and (43) in both (2) and (7) gives the following mathematical equations for system parameter identification:

$$(m_i - X_{\dot{u}i})\dot{u}_i - X_{ui}u_i = \tau_{xi} \tag{44}$$

$$(m_i - Y_{\dot{v}i})\dot{v}_i - Y_{vi}v_i = \tau_{yi} \tag{45}$$

$$(I_{zi} - N_{\dot{r}i})\dot{r}_i - N_{ri}r_i = \tau_{\psi i} \tag{46}$$

The vessel motion data is obtained by pulling the vessel in the surge, sway, and yaw direction several times as shown in Fig. 7. Once the load cell measures the amplitude of the pulling force, the load cell amplifier is then used for signal conditioning such that the signal can be amplified and converted into an output value. The analog input module and real-time controller take and save these values. The host computer collects these pulling force data via a wireless router. Motions in the x and y directions and rotation about the z-axis are obtained using the camera system.

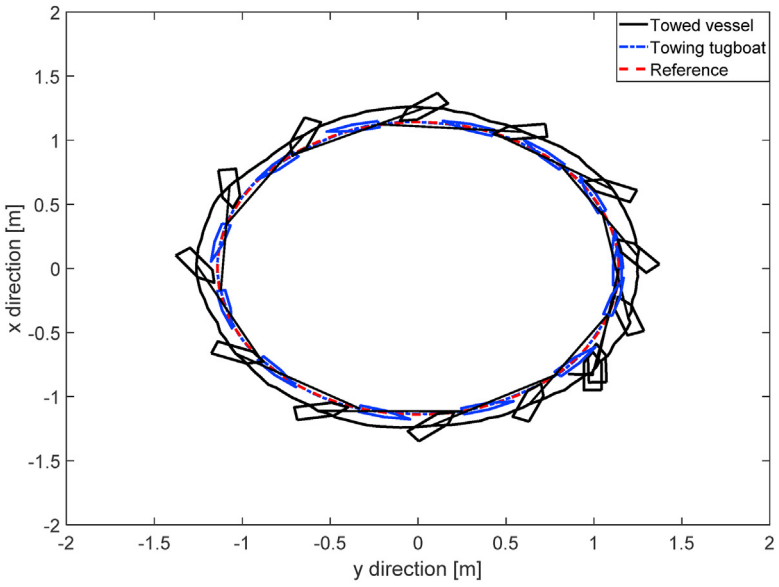
Fig. 8(a) shows the obtained data of the pulling force and motion of the towed vessel in the x direction. Calculating the parameters of the inertia and damping matrices is done as follows. For instance, considering the surge motion, then Eq. (40) is used to estimate parameters $m_2 - X_{\dot{u}2}$ of the system inertia matrix M_2 and X_{u2} of the damping matrix D_2 (Fossen, 2002; Tran and Kim, 2016; Oh et al., 2010; Skjetne et al., 2004; Nguyen et al., 2018). The measured pulling force data is fed into τ_{x2}. Also, Fig. 8(a) show the fitting results of the experiment and simulation tests, where the 'GoodnessOfFit' function in Matlab is employed to evaluate the data fitting accuracy.

And, Fig. 8(b ~ c) illustrate, respectively, the obtained data of the pulling forces and motions of the towed vessel in the y direction and yaw angle.

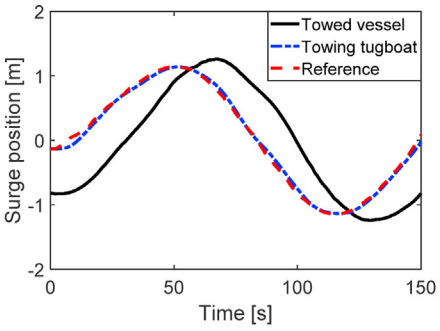
Based on this method, all data of surge, sway, and yaw motions are obtained from experiment trials. To obtain reliable and accurate data, we performed several experiment tests (More than ten times.) Using the experiment results, the unknown parameters in the hydrodynamic matrix M_i and D_i are calculated. After several iterations, the partially unknown hydrodynamic matrix M_i and D_i are obtained as shown in Eqs. 47–50:

$$M_1 = \begin{bmatrix} m_1 - X_{\dot{u}1} & 0 & 0 \\ 0 & m_1 - Y_{\dot{v}1} & 0 \\ 0 & 0 & I_{z1} - N_{\dot{r}1} \end{bmatrix} = \begin{bmatrix} 13.5588 & 0 & 0 \\ 0 & 11.0324 & 0 \\ 0 & 0 & 0.22559 \end{bmatrix} \tag{47}$$

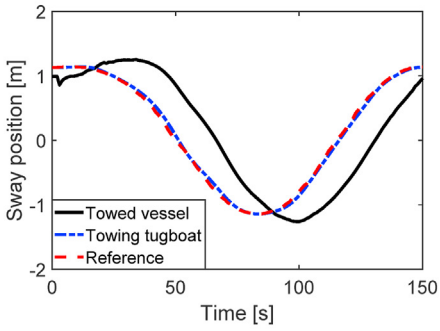
$$D_1 = \begin{bmatrix} -X_{u1} & 0 & 0 \\ 0 & -Y_{v1} & 0 \\ 0 & 0 & -N_{r1} \end{bmatrix} = \begin{bmatrix} 0.5882 & 0 & 0 \\ 0 & 1.47059 & 0 \\ 0 & 0 & 0.05222 \end{bmatrix}, \tag{48}$$



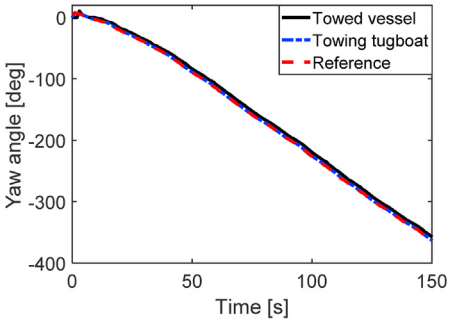
(a) turning route tracking performances



(b) surge motions



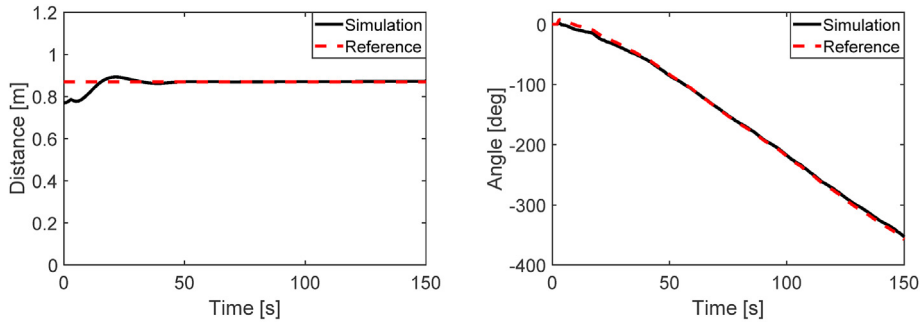
(c) sway motions



(d) yaw angles

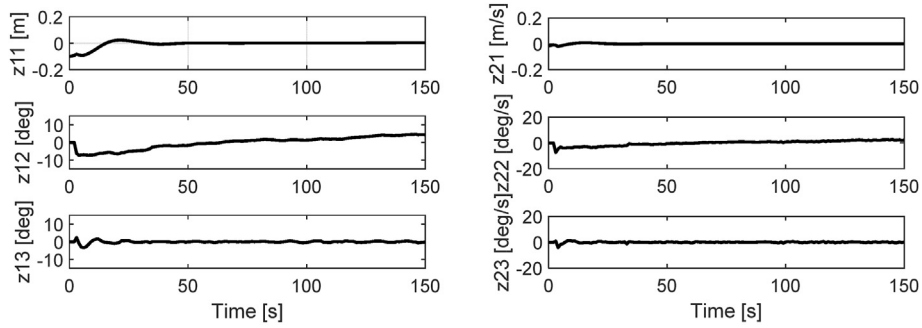
Fig. 9. Simulation results of the two vessels' motions.

$$M_2 = \begin{bmatrix} m_2 - X_{\dot{u}2} & 0 & 0 \\ 0 & m_2 - Y_{\dot{v}2} & 0 \\ 0 & 0 & I_{z2} - N_{\dot{r}2} \end{bmatrix} = \begin{bmatrix} 13.2409 & 0 & 0 \\ 0 & 13.5285 & 0 \\ 0 & 0 & 0.2869 \end{bmatrix}, \tag{49}$$



(a) distance (b) angle

Fig. 10. The relative motions between the tugboat and the towed vessel acquired with simulation tests.



(a) errors in distance and degree (b) errors in velocity and angular velocity

Fig. 11. The calculated error dynamics from Eqs. (27) and (28) in simulation mode.

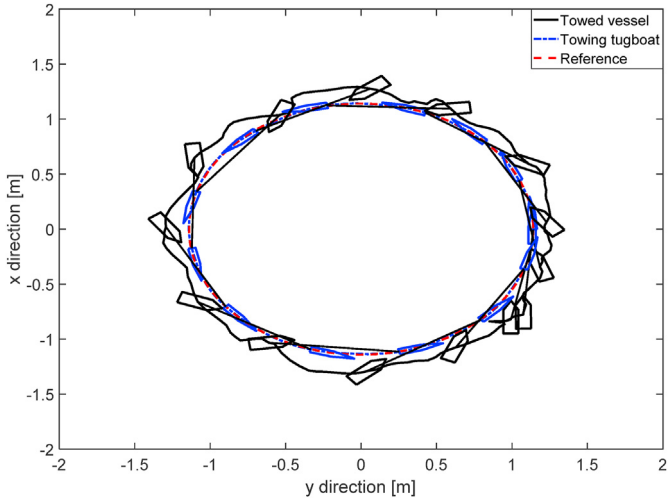


Fig. 12. Simulation results of the motion of the two vessels without control.

Table 2
The unknown parameters of inertia and damping matrices.

Case no.	Δm	Δd
Case 0	0	0
Case 1	$0.4M_{3.3}$	$0.2D_{3.3}$
Case 2	$-0.4M_{3.3}$	$-0.2D_{3.3}$

$$D_2 = \begin{bmatrix} -X_{u2} & 0 & 0 \\ 0 & -Y_{v2} & 0 \\ 0 & 0 & -N_{r2} \end{bmatrix} = \begin{bmatrix} 0.6246 & 0 & 0 \\ 0 & 1.6260 & 0 \\ 0 & 0 & 0.0392 \end{bmatrix}. \tag{50}$$

4.2. Simulation results

Here we investigate the tracking performance of the towed vessel. As abovementioned, the tracking route of the towed vessel is produced by the towing tugboat. The towing tugboat follows the defined target trajectory such that the tracking route for the towed vessel is generated.

The PID control gains of the towing tugboat were chosen as:

$$K_{P1} = diag\{\, 0.1230 \quad 0.1992 \quad 0.0117 \,\} \tag{51}$$

$$K_{I1} = diag\{\, 0.0018 \quad 0.0044 \quad 0.0038 \,\} \tag{52}$$

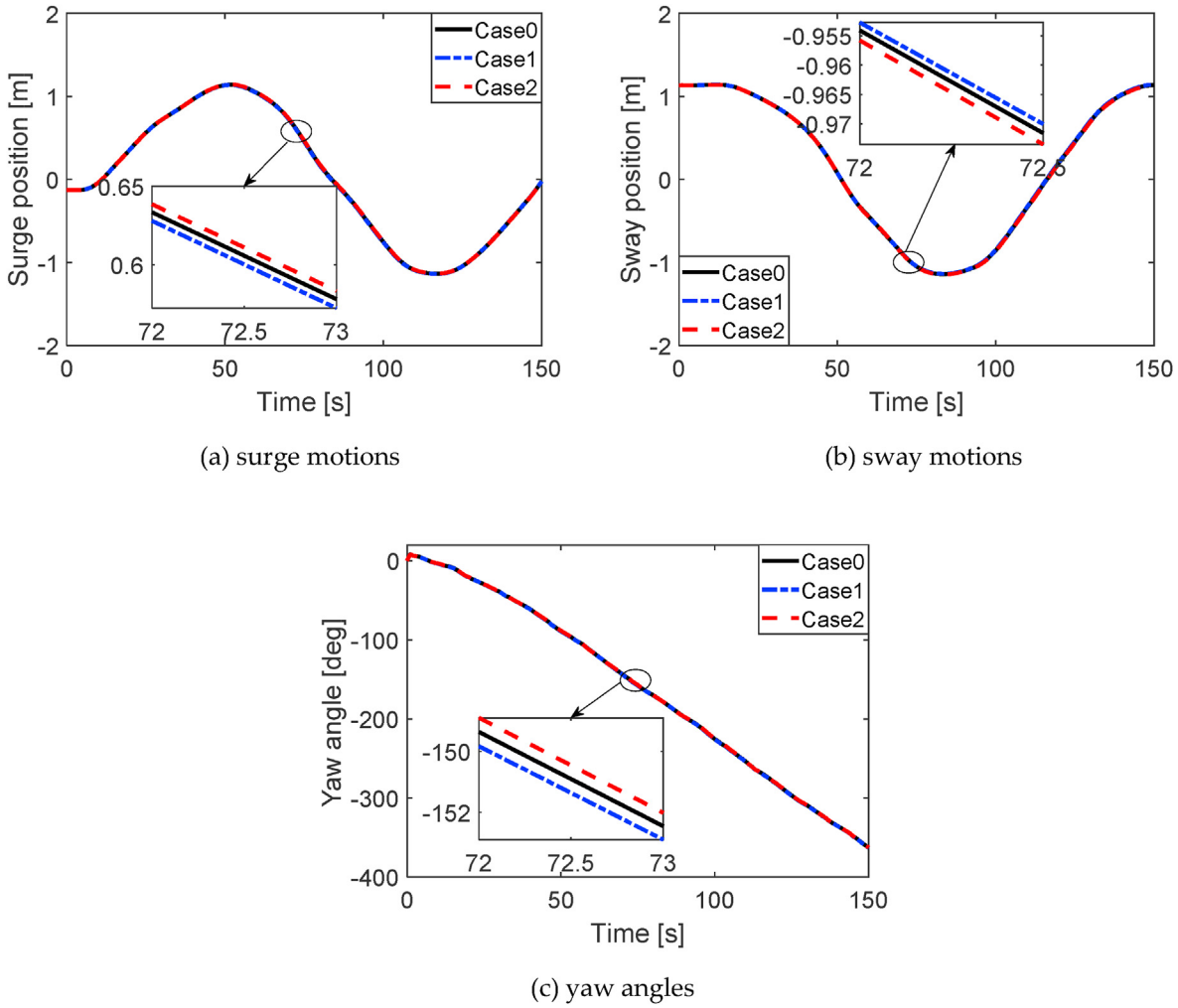
$$K_{D1} = diag\{\, 0.0928 \quad 0.2210 \quad 0.1920 \,\} \tag{53}$$

The back-stepping control gains of the towed vessel were calculated as:

$$K_{P2} = diag\{\, 0.1140 \quad 0.1385 \quad 0.0505 \,\} \tag{54}$$

$$K_{D2} = diag\{\, 0.0160 \quad 0.0139 \quad 0.0050 \,\} \tag{55}$$

$$\Lambda = diag\{\, 0.9500 \quad 0.6925 \quad 0.2523 \,\} \tag{56}$$



(a) surge motions

(b) sway motions

(c) yaw angles

Fig. 13. Motions of the towing tugboat with unknown parameters.

The obtained control gains preserve system stability, and the effectiveness of the proposed control strategy is now verified by performance analysis of both simulation and experimental tests. In this study, due to space constraints of the experiment setting, we considered a circle-type reference signal with a radius of 1.175 [m], and the reference distance between the two vessels of 0.87 [m].

Based on the stated conditions, simulations and experimental tests were conducted, and the results are illustrated in the following figures.

First, the simulation results are presented in Figs. 9–12. Fig. 9 (a) shows the response of the towing and towed vessels following a circular trajectory. The dashed line is the reference trajectory, the dashed-dot line is the moving route and the heading angle of the towing vessel, whereas the solid line indicates the motion of the towed vessel. On the other hand, Fig. 9 (b)~(d) show the surge, sway motions, and yaw angles of the two vessels, respectively. Relative motions between the tugboat and the towed vessel are shown in Fig. 10. The dashed line is the relative reference, whereas the solid line indicates the relative response. The relative distance is shown in Fig. 10 (a), while Fig. 10 (b) shows the relative heading angle. The error dynamics z_1 and z_2 defined in Eqs. (27) and (28) are shown in Fig. 11. The distance error z_{11} is minor and in the neighborhood of zero. The angle errors z_{12} and z_{13} are smaller than 7 [degree]. The simulation result without control of the towed vessel under the same condition as Fig. 9 is shown in Fig. 12. Since the rudders are not operated, it shows the unstable motion of the towed vessel regardless of the tugboat route.

The simulation results highlight the performance of the proposed strategy. Especially, the trajectory tracking performance of the towed vessel is good. Relative motions between the tugboat and the towed vessel are kept under control.

In fact, from the identification process (chapter 4.1), the inertia and damping matrices were simplified by eliminating elements that are unknown parameters of the system. Therefore, it is necessary to investigate the performance of the control system with the presence of unknown parameters.

To evaluate the effect of unknown parameters, the inertia matrix and damping matrix with unknown parameters are given as the following

$$M_i = \begin{bmatrix} m_i - X_{\dot{u}i} & 0 & 0 \\ 0 & m_i - Y_{\dot{v}i} & \Delta m \\ 0 & \Delta m & I_{zi} - N_{\dot{r}i} \end{bmatrix} \tag{57}$$

$$D_i = \begin{bmatrix} -X_{ui} & 0 & 0 \\ 0 & -Y_{vi} & \Delta d \\ 0 & \Delta d & -N_{ri} \end{bmatrix}, \; i = 1, 2. \tag{58}$$

where Δm and Δd are described in Table 2. The range of unknown parameters is limited to a specific percentage of the 3rd row and

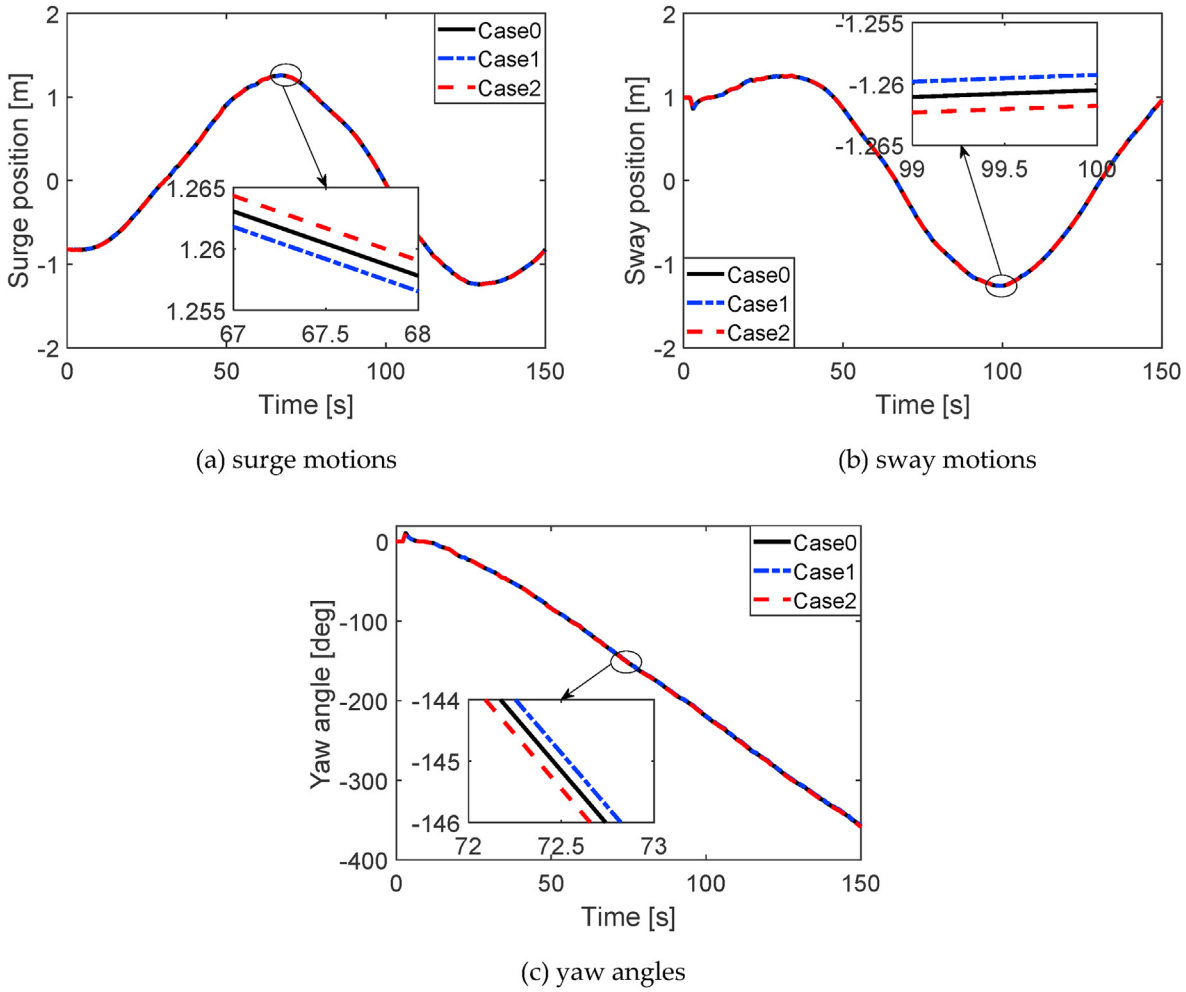


Fig. 14. Motions of the towed vessel with unknown parameters.

3rd column of each matrix (see Table 2).

Based on these considerations, the simulations are conducted using the newly defined parameters, where the other conditions are similar to the nominal plant simulation case.

Figs. 13 and 14 show the simulation result with unknown parameters. Fig. 13 represents the motion of the towing tugboat; Fig. 14 depicts the tracking performance of the towed vessel. Figures (a)~(c) of both Figs. 13 and 14 illustrate, respectively, the surge and sway motions, and the yaw angle of the vessel. The distance error between the three cases is very small and can be neglected. Therefore, the control performance with the presence of unknown parameters is validated with simulation tests.

5. Experiment

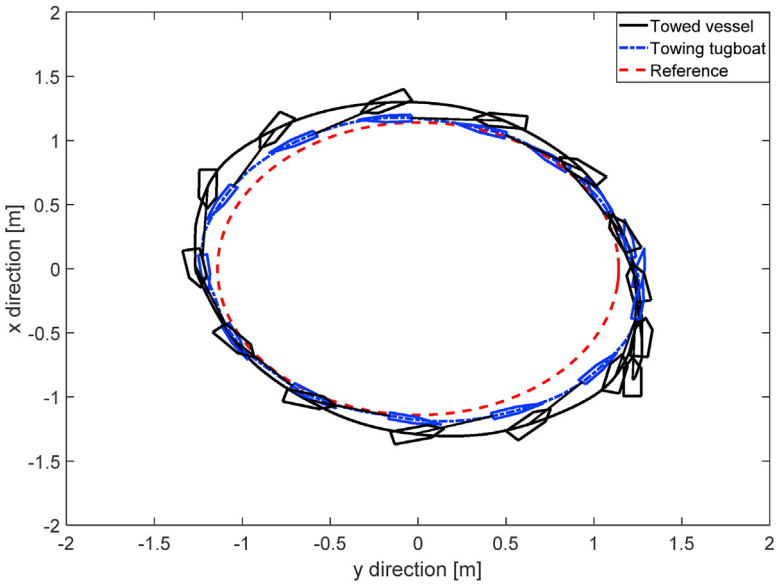
Following the same procedure as the simulation study, Figs. 15–19 show experimental results where the reference is the same as the simulation tests. The control laws developed in Eq. 51–56 are applied to the towing vessel system. Fig. 15 (a) shows the tracking performance following the circular route, while Fig. 15 (b) ~(d) illustrate, respectively, the surge motion, the sway motion, and the yaw angles of the two vessels. The relative distances are shown in Fig. 16 (a), while Fig. 16 (b) shows the relative heading angles. And, the error dynamics z_1 and z_2 are shown in Fig. 17, while the distance error z_{11} is small and in the neighborhood of zero. The angle errors z_{12} and z_{13} are smaller than 10 [degree].

To highlight the effectiveness of the proposed control strategy, experimental tests were conducted with an uncontrolled towed vessel. Fig. 18 shows the experimental result without control of the towed vessel under the same condition as Fig. 15. Since the rudders are not controlled, the motion of the towed vessel is unstable compared to the controlled case.

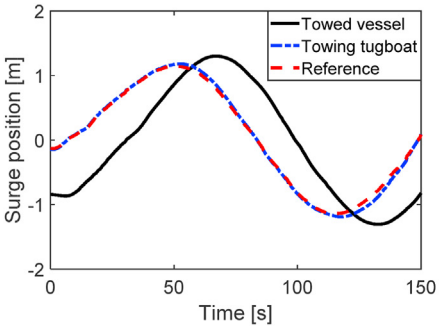
Fig. 19, especially, compares the error dynamics z_1 of the uncontrolled and controlled cases. Whilst the maximum value in the uncontrolled case of the distance error z_{11} is 0.1343 [m] at 128.7 [s], the controlled case records 0.0567 [m] at 87.9 [s]. The initial state error in the controlled case is larger than in the uncontrolled case. Concerning the angle errors z_{12} and z_{13}, these errors are larger in the uncontrolled case than in the controlled case. We can observe a definite difference between the two experimental results. More importantly, the route tracking performance of the towed vessel has improved significantly.

From the simulation and experimental results, the towed vessel can follow the towing tugboat adequately and in a stable manner. This proves that the proposed control strategy works well and it is applicable in the real field.

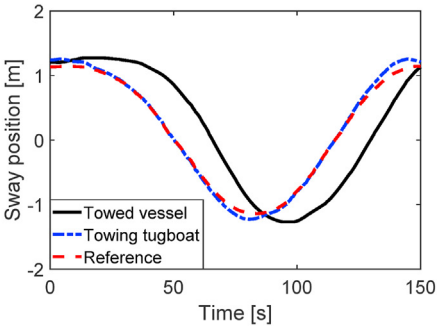
Finally, it was confirmed through this study that more stable and superior sailing performance can be secured with minimal control function if the towed vessel's rudder is activated.



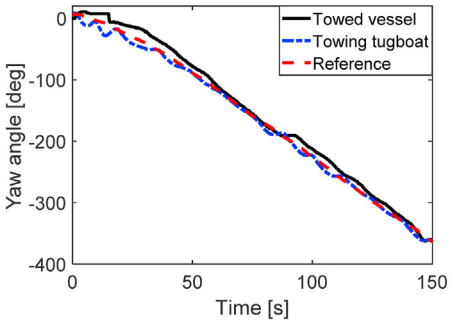
(a) turning route tracking performances



(b) surge motions



(c) sway motions



(d) yaw angles

Fig. 15. Experimental results of the two vessels' motions.

6. Conclusion

In this study, the authors have considered the control problem of the towing system consisting of two vessels and proposed a new method to solve this critical issue. The vessels are connected with rope and work as the leader and follower during towing operation. The towing vessel has the power propulsion system, while the towed vessel is connected to the leader and does not have any active system except the rudder. Therefore, safe sailing and robust maneuvering are not preserved. If the towing vessel system is exposed to harsh environmental conditions, a serious collision accident may occur. To overcome this issue, the authors proposed a new control strategy providing the rudder with an active role in the towed vessel. In this system configuration, the rudders are appropriately installed on the towed vessel, such that the towed vessel can guarantee safe sailing and maintain good tracking of the course generated by the tugboat. For future works, designing a system that helps cope with un-modeled external forces and moments due to

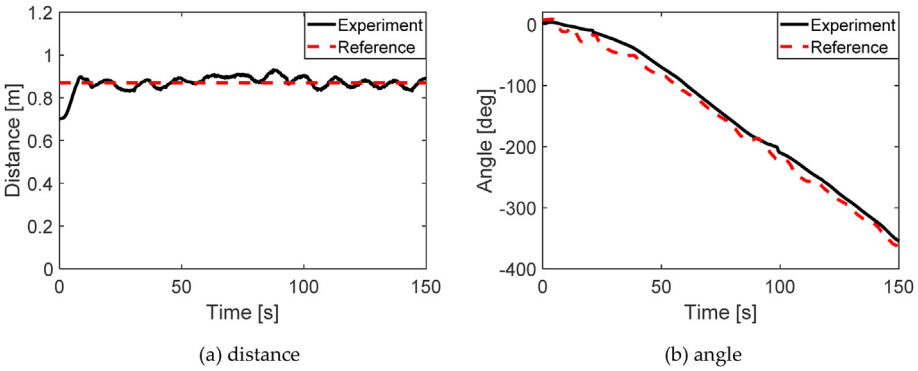


Fig. 16. Experimentally obtained relative motions between the towing and the towed vessels.

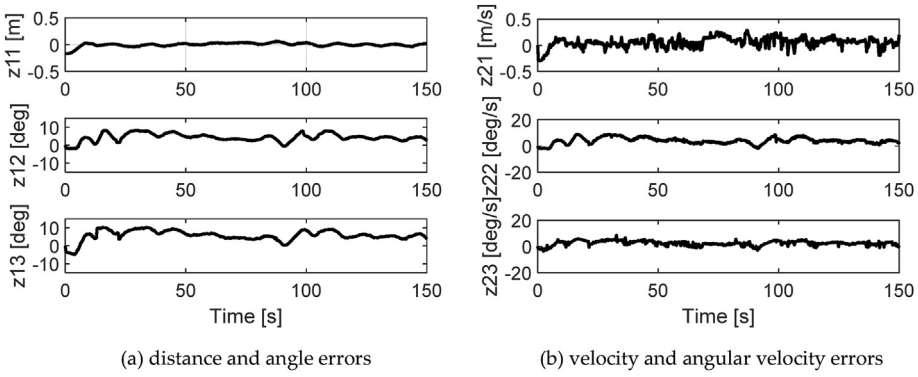


Fig. 17. The calculated error dynamics from Eqs (27) and (28) in experimental mode.

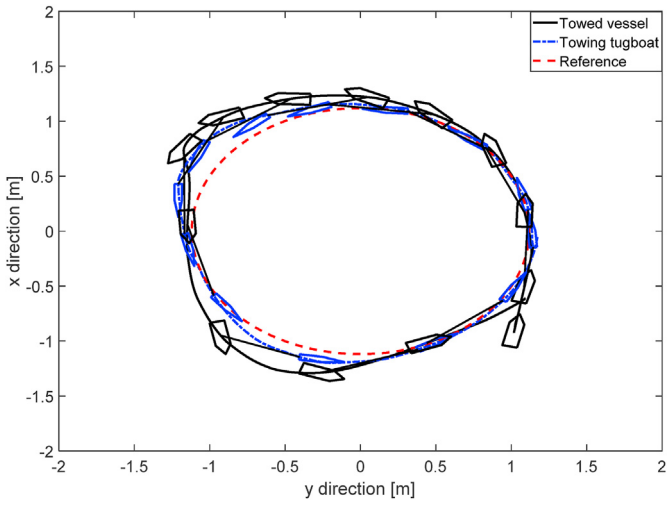


Fig. 18. Experimental results of the two vessels without control.

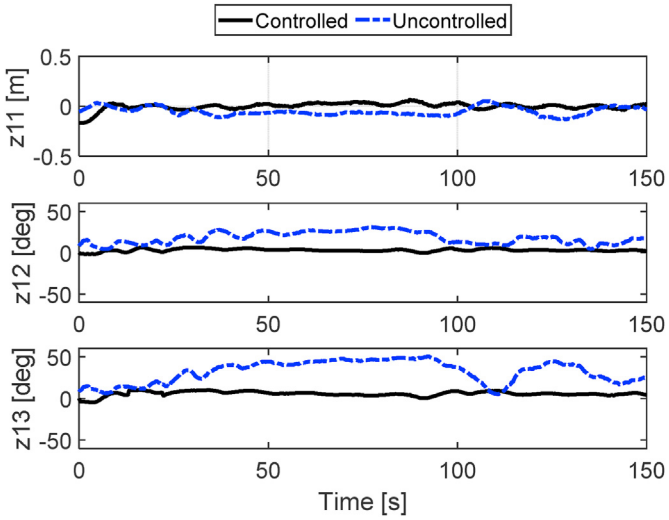


Fig. 19. Error dynamics comparison between the controlled and uncontrolled cases.

harsh sea conditions is one of the main objectives.

The full mathematical model of the two connected vessels has been obtained, and a nonlinear back-stepping controller is applied in simulation and experimental study. The simulation and experimental results demonstrate that the proposed control strategy preserves an accurate tracking performance and safe sailing of the towed vessel.

Declaration of competing interest

The authors declare that they have no known competing financial interests or personal relationships that could have appeared to influence the work reported in this paper.

Acknowledgement

This work was supported by a Research Grant of Pukyong National University(2019).

References

Bui, V.P., Kim, Y.B., 2011. Development of constrained control allocation for ship berthing by using autonomous tugboats. Int. J. Contr. Autom. Syst. 9 (6), 1203–1208.

Bui, V.P., Jeong, J.S., Kim, Y.B., Kim, D.W., 2010. Optimal control design for automatic ship berthing by using bow and stern thrusters. Journal of Ocean Engineering and Technology 24 (2), 10–17.

Bui, V.P., Kawai, H., Kim, Y.B., Lee, K.S., 2011. A ship berthing system design with four tug boats. J. Mech. Sci. Technol. 25 (5), 1257–1264.

Dong, Z., Wan, L., Li, Y., Liu, T., Zhang, G., 2015. Trajectory tracking control of underactuated USV based on modified backstepping approach. International Journal of Naval Architecture and Ocean Engineering 7 (5), 817–832.

Fang, M.C., Lee, Z.Y., 2016. Application of neuro-fuzzy algorithm to portable dynamic positioning control system for ships. International Journal of Naval Architecture and Ocean Engineering 8 (1), 38–52.

Fitriadhy, A., Yasukawa, H., Koh, K.K., 2013. Course stability of a ship towing system in wind. Ocean. Eng. 64, 135–145.

Fossen, T.I., 2002. Marine Control System-Guidance, Navigation, Rigs and Underwater Vehicle. Norwegian University of Science and Technology, Trondheim, Norway.

Kawai, H., Kim, Y.B., Choi, Y.W., 2009. Anti-sway system with image sensor for container cranes. J. Mech. Sci. Technol. 23 (10), 2757–2765.

Kawai, H., Kim, Y.B., Choi, Y., 2012. Measurement of a container crane spreader under bad weather conditions by image restoration. IEEE Transactions on Instrumentation and Measurement 61 (1), 35–42.

Kehtarnavaz, N., Kim, N., 2005. Digital Signal Processing System-Level Design Using Labview.

Kunimitsu, S., Asama, H., Kawabata, K., Mishima, T., 2004. Development of crane vision for positioning container. J. Robot. Mechatron. 16 (2), 186–193.

Lee, D.J., Kim, J.K., Kim, B.S., 2000. Design of an automatic winch system for small fishing vessel. Journal of the Korean Society for Fisheries and Technology 36 (3), 157–165.

Lopez, M.J., Rubio, F.R., 1992. LQG/LTR control of ship steering autopilots. Proceedings of the 1992 IEEE International Symposium on Intelligent Control 447–450.

Michiel, W., Erjen, L., Kristin, Y.P., Henk, N., 2011. Output feedback tracking of ships. IEEE Trans. Contr. Syst. Technol. 19 (2), 442–448.

Nguyen, V.T., Choi, Y.W., Yoon, J.I., Choi, K.H., Son, C.H., Kim, Y.B., 2018. Modeling, identification, and simulation of positional displacement control for ribbon bridges. In: MATEC Web of Conferences IJCAET & ISAMPE 2017, p. 159.

Oh, S., Sun, J., Li, Z., a Celkis, E., Parsons, D., 2010. System identification of a model ship using a mechatronic system. IEEE ASME Trans. Mechatron. 15 (2), 316–320.

Skjetne, R., Smogeli, Ø.N., Fossen, T.I., 2004. A Nonlinear Ship Maneuvering Model: identification and adaptive control with experiments for a model ship. Model. Ident. Contr. 25 (1), 3–27.

Tran, A.M.D., Kim, Y.B., 2016. Dynamic identification and robust control performance evaluation of towing rope under rope length variation. Journal of the Korean Power System Engineering 20 (2), 58–65.

Tran, A.M.D., Ji, S.W., Kim, Y.B., 2014. A ship berthing system design by cooperating with tugboats and dampers. Journal of Drive and Control 11 (3), 7–13.

Tran, D.Q., Lee, D.H., Kim, T.W., Kim, Y.B., Park, H.C., 2018. A study on maneuvering performance improvement of a towed vessel without a power propulsion system: system modeling. Journal of the Korean Society of Fisheries and Ocean Technology 54 (4), 343–352.

Tran, D.Q., Suh, J.H., Kim, Y.B., 2019. Leader-following control system design for a towed vessel by tugboat. Journal of Ocean Engineering and Technology 33 (5), 462–469.

Wang, J.Q., Zou, Z.J., Wang, T., 2019. Path following of a surface ship sailing in restricted waters under wind effect using robust H_∞guaranted cost control. International Journal of Naval Architecture and Ocean Engineering 11 (1), 606–623.

Wang, Y., Chai, S., Nguyen, H.D., 2020. Experimental and numerical study of autopilot using Extended Kalman Filter trained neural networks for surface vessels. International Journal of Naval Architecture and Ocean Engineering 12, 314–324.

Yamato, H., Uetsuki, H., Koyama, T., 1990. Automatic berthing by the neural controller. Proc. 9th Ship Control Systems Symposium USA 3, 183–201.

Yoon, H.J., Hwang, Y.C., Cha, E.Y., 2010. Real-time container position estimation method using stereo vision for container auto-landing system. In: ICCAS 2010 - International Conference on Control, Automation and Systems, pp. 872–876.

Zhang, Y., Hearn, G.E., Sen, P., 1999. A multivariable neural controller for automatic ship berthing. Journal of IEEE Control System 17, 31–44.

Zwierzewicz, Z., 1999. On the ship trajectory tracking LQG controller design. Transactions on the Built Environment 42, 399–406.